PRODUCTION OF ULTRAFINE-GRAINED TITANIUM BY INDUSTRIAL CALIBER ROLLING

G. Krállics [1], J. Gubicza [2], Z. Bezi [3]

[1] Budapest University of Technology & Economics
Department of Materials Science and Engineering
Budapest, Hungary
krallics@eik.bme.hu
[2] Eötvös Loránd University
Department of Materials Physics
Budapest, Hungary
[3] Bay Zoltán Nonprofit Ltd. for Applied Research
Engineering Division
Budapest, Hungary

Accepted October 19, 2015

Abstract

The possibility of mass production of ultrafine-grained (UFG) titanium by industrial caliber rolling was examined. As complementary investigations, laboratory caliber rolling tests were also performed. The mechanical and metallurgical characteristics of the rolled materials were studied. The process led to an UFG microstructure with high dislocation density, accompanied by high tensile strength and good ductility. Mathematical modeling indicated that the refinement of the grains was caused by the large shear strains and the non-monotonicity of deformation, i.e. caliber rolling can be regarded as a severe plastic deformation procedure. In addition, the characteristics of the samples processed by industrial caliber rolling were compared to those produced under laboratory conditions. The microstructure and the mechanical properties of the materials processed by the two ways were similar, indicating that industrial caliber rolling is capable of mass production of UFG titanium.

1. Introduction

In the past decades, several severe plastic deformation (SPD) procedures were developed for processing bulk metallic materials with ultrafine-grained (UFG) microstructure. Accumulative roll bonding (ARB) [1, 2], equal channel angular pressing (ECAP) [3, 4], high pressure torsion (HPT), [5] and repetitive corrugation and straightening [6] are some examples for these processes. SPD procedures usually produce UFG materials under laboratory conditions, i.e. their productivity is low. Significant breakthrough in the application of UFG materials (i.e. their commercialization) can only be achieved if they were manufactured in an industrial environment.

The common characteristic of the SPD techniques is the large shear strain and the non-monotonic nature of the deformation. The concept of monotonic deformation was introduced

by [7]. As he wrote, a forming process develops monotonically if no component of the rate of strain tensor changes its sign, i.e. the eigenvectors of the rate of strain tensor are parallel to the eigenvectors of the strain tensor during the whole deformation process and the Lode parameter remains constant. Studying the possible ways of deviation from the monotonic deformation contributes to develop processes which assure the production of fine grains. Although, caliber rolling is not an usual SPD method, its industrial application for producing UFG titanium is promising due to its productivity and non-monotonic nature.

According to former experience, titanium is an ideal material for devices to be implanted into the human body. It is chemically inert, does not react with human body fluids, and, if it is necessary, after proper surface treatment the bone is able to adhere to titanium implants. However, if the adherence of the implant to the bone is contraindicated, it can be impeded by tailoring the titanium surface morphology. This dual feature makes this metal well and widely applicable for different medical purposes.

Besides the listed favourable biological properties, titanium makes possible the application of up-to-date diagnostic procedures (e.g. Magnetic Resonance Imaging (MRI) and Computer Tomography (CT)) on persons having titanium implants, because it does not show magnetic properties in strong magnetic fields and does not interfere with X-ray radiation. These statements apply for titanium alloys, as well.

From the physiological viewpoint, pure titanium is better than its alloys since the alloying elements may yield toxic reactions in the human body. At the same time, the strength of pure titanium is much lower than that of its alloyed counterparts. In pure metals the strength can be improved by grain refinement with the application of SPD procedures, resulting in high strength semi-products for the fabrication of implants and protheses. The usage of pure titanium significantly decreases the risk of irritations caused by the alloying elements, therefore the implant might stay in the body if the risk of removal is too high. While medical application of titanium alloys is widespread universally, examples for the application of commercial purity (CP) titanium are rare. Further, there is no solution yet for the industrial mass production of bulk UFG titanium. The present paper studies the microstructure and the mechanical properties of CP-Ti processed by caliber rolling in both laboratory and industrial environments. The degree of non-monotonicity for these procedures is also investigated. It is found that caliber rolling may be a candidate for mass production of UFG CP-Ti for medical applications.

2. Experiments and process modeling

2.1. Rolling experiments in laboratory and industry

Grade 2 titanium specimens with 200 mm in length and 30 mm in diameter in an annealed condition (annealing at 650 °C for 2 h then cooling in air) were used for the laboratory rolling tests. The initial mechanical properties were as follows: *yield strength,* YS = 332 MPa, ultimate tensile strength, UTS = 439 MPa, reduction in area, Z = 58 %, elongation to failure, A = 22 %, strain energy density to fracture, W_f = 412 J / cm^3.

The laboratory caliber rolling was carried out on samples pre-heated to 450 °C. A twin-motor rolling mill with the power of 2 × 7.5 kW was used in the experiments. The diameter of the roll was 180 mm. The roll stand can be used in both symmetrical and asymmetrical modes (see **Figure 1**). The first mode enables both flat and caliber rolling processes. The caliber rolls

used in the present study are shown in **Figure 2**. Four reductions were performed in the first part of the process. The roll speed was 6 rpm. After the first part of the rolling procedure the specimen was reheated to 450 °C. The second part of the rolling process was performed in six passes using the same heating procedure between subsequent passes as applied in the first part of the process. In the first and second parts of the procedure different roll pairs were used, as shown in **Figure 2**. After the last pass in the second part a final diameter of 8 mm was achieved.

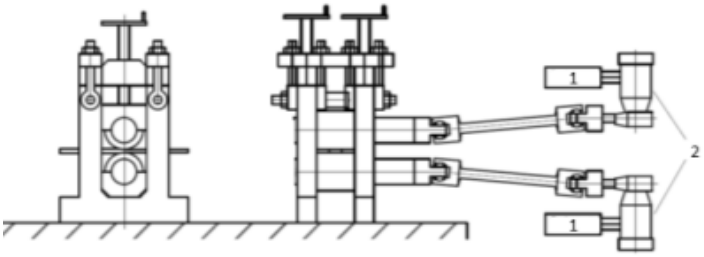

Figure 1. The sketch of the experimental roll stand for caliber rolling. 1 – speed control, 2 – twin motor drive.

Figure 2. The pairs of rolls.

Industrial warm caliber rolling of titanium was performed using the rolling mill system of OAM Ózd Steelworks Ltd. (Ózd, Hungary). The shape and the size of the roll cavities for the twelve passes are shown in **Figure 3** and **Table 1**. At the beginning of the process the material was heated to the rolling temperature of ~ 300 °C in an induction furnace. This temperature was lower than that applied for laboratory rolling, since the heat production rate during industrial rolling was larger due to the higher rolling speed. During the rolling process the "elongation section" was executed in the first six mill stands. The speed of the first pair of rolls was 8 rpm. The finish rolling was performed in the next six stands. The diameter of the rolls was 415 mm. The oval piece was rotated by 90 ° at each stand in order to arrive in the next mill position. The bars with 1000 mm in length were continuously moved through the six mill stands. The temperature was measured by contact thermometers. The cross section of the bar was reduced from 70 to 34 mm during the elongation section of rolling. The process parameters are listed in **Table 2**. The rolled bars were cut to smaller pieces with 2000 mm in length. They were heated to ~ 300 °C before the finish rolling. In this final step of processing the diameter of the bars was reduced from 34 to 20 mm. The process parameters for finish rolling are listed in **Table 3**. The speed of the first pair of rolls in the finish rolling process was 40 rpm which is larger than in the case of the elongation section of rolling.

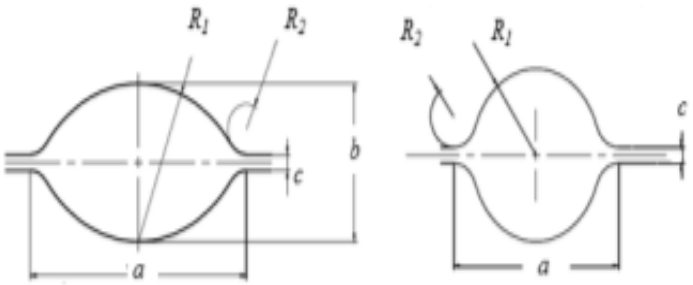

Figure 3. The shape and the size of the roll cavities (left side odd, right side even ones).

Table 1. The size of the roll cavities for the twelve passes applied in industrial caliber rolling.

Cavity No	*a* mm	*b* mm	*c* mm	R_1 mm	R_2 mm	Cavity No	*a* mm	*c* mm	R_1 mm	R_2 mm
1	91.73	50	5	50	8	2	71.77	5	29	10
3	74.13	48	5	40	8	4	57.63	5	22,5	7
5	60.79	32	4	32	8	6	43.48	3	17	6
7	49.18	25	3	27	6	8	37.08	3	14	6
9	40.18	20	3	22	6	10	31.62	3	11,5	6
11	32.98	18	2	16	5	12	31.44	2	10	5

Table 2. Parameters of elongation rolling (∅ 70 → ∅ 34 mm).

Pass No.	Stretching factor	Maximum roll force [kN]	Maximum roll torque [Nm]	Temperature [°C]
1	1.26	1100	36000	420
2	1.24	920	28000	435
3	1.26	950	27000	446
4	1.23	845	21000	452
5	1.28	810	19000	440
6	1.23	600	14500	460

Table 3. Parameters of finish rolling (∅ 34 → ∅ 20 mm).

Pass No.	Stretching factor	Maximum roll force [kN]	Maximum roll torque [Nm]	Temperature [°C]
7	1.2	700	15500	485
8	1.26	510	10500	495
9	1.22	550	8500	523
10	1.22	425	6000	460
11	1.14	380	3500	480
12	1.15	260	3200	515

The industrial manufacturing process resulted in four products. The first two ones were obtained by caliber rolling. The third and fourth product was obtained by the combination of caliber and flat rolling processes.

Table 4. The rolled industrial products.

Products	Elongation rolling	Finish rolling	Cold rolling
1	∅70 ⇒ ∅34 mm / 6 passes	∅34 ⇒ ∅20 mm / 6 passes	
2	∅70 ⇒ ∅34 mm / 6 passes	∅34 ⇒ ∅20 mm // 6 passes	∅20 ⇒ ∅18 mm / 2 passes
3	∅70 ⇒ ∅34 mm / 6 passes	∅34 ⇒ □14×45 mm /2 passes	
4	∅70 ⇒ ∅34 mm /6 passes	∅34 ⇒ □14×45 mm /2 passes	□14x45 ⇒ □7×51 mm /1 pass

In order to improve the quality of the surface and the dimensional accuracy in addition to increasing the strength of the rods further cold rolling was performed. In this process the

diameter was reduced by about 2 mm with a scattering of about 1 mm. The flat bars were further reduced to 7 mm thickness. Their width increased to 51 mm. The processing history of the four industrially manufactured samples is listed in **Table 4**.

It should be noted that that the shape and size of cavities in the laboratory rolling procedure were designed in order to obtain similar deformation and thermal conditions as in the industrial environment. For instance, the average equivalent strains calculated for the whole volume of the material after the laboratory and the industrial caliber rolling procedures were 2.64 and 2.50, respectively.

2.2. Modelling the strain path of the rolling process

Finite element modelling (FEM) was employed to analyse the caliber rolling process theoretically. The details of FEM procedure can be found in [8]. In the present work the objective of the modelling was to demonstrate the cyclic nature of the process, indicating that it is non-monotonic, resulting in fine grains. The permanent deformation of the samples is demonstrated by the strain trajectory approach as initiated by [9], representing the deviatoric strain tensor (e) in a five-dimensional vector space as:

$$e_1 = \sqrt{\frac{3}{2}} \ln V'_{11},\ e_2 = \sqrt{2}\left(\ln V'_{22} + \frac{1}{2} \ln V'_{11} \right), \qquad (1)$$
$$e_3 = \sqrt{2} \ln V'_{12},\ e_4 = \sqrt{2} \ln V'_{23}, e_5 = \sqrt{2} \ln V'_{31}$$

where $\ln \mathbf{V}'$ is the logaritmic deviatoric strain tensor. Some examples for the strain trajectories are shown in **Figure 4**.

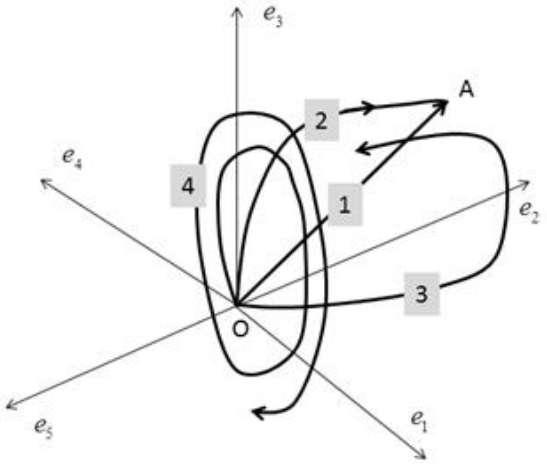

Figure 4. Examples for the strain trajectories in the five dimensional vector space.

In **Figure 4** trajectory #1 is monotonic, #2 is nearly monotonic, # 3 is simple non-monotonic and #4 is cyclic non-monotonic. In order to appreciate the measure of the non-monotonicity of deformation, consider the nearly monotonic trajectory #2 [10]. During deformation the end-point of the strain vector travels along the curved OA trajectory. The ideally monotonic deformation corresponds to the straight line OA. Therefore, at the deformation time, t, the measure of non-monotonicity is given as:

$$NM(t) = \frac{\bar{\varepsilon}(t)}{\bar{\varphi}(t)} \geq 1, \qquad (2)$$

where $\bar{\varepsilon}$ is the total equivalent strain, which is equivalent to the length of the trajectory, $\bar{\varphi}$ is the equivalent logarithmic strain, which equals the length of the straight trajectory OA. In the

case of non-monotonic deformation the complete trajectory is separated into n nearly monotonic portions.. For each part the $(NM)_i$ is determined as the ratio of the length of the local trajectory part and the straight segment connecting its end points. In this case the measure of non-monotonicity of the whole deformation is given as:

$$NM = \sum_{i=1}^{n} (NM)_i . \quad (3)$$

The larger the value of NM, the higher the degree of non-monotonicity of deformation. It should be noted that although all $(NM)_i$ values are larger than one, NM may decrease with increasing strain as the end points of the segments may vary during the development of the deformation trajectory.

2.3. Material testing

The mechanical properties of the rolled materials were investigated by tensile test using an Instron universal mechanical testing machine (type 8809) at room temperature and the cross-head velocity of 6 mm / min. The tests were carried out on cylindrical specimens with the length and diameter of 25 and 5 mm, respectively, machined out of the rolled bars. For both laboratory and industrial rolling 3 – 3 samples were tested under the same conditions.

The grain structure in the initial and the rolled specimens was examined by a Tecnai G2 X-TWIN transmission electron microscope (TEM). The TEM foils were prepared from both the cross- and longitudinal sections of the rods which were thinned by mechanical grinding to a thickness of 20 – 40 μm. The foils were further thinned by Ar-ion milling using a Gatan Model 691 precision ion polishing system. The microstructures of the initial and the rolled samples were also examined by X-ray line profile analysis. Before measurements the surface was mechanically polished to a mirror finish with diamond paste. The surface layer, distorted during polishing, was removed by chemical etching using hydrogen fluoride. The measurements of the X-ray diffraction lines were performed on the longitudinal sections using a special high-resolution diffractometer with Co $K\alpha_1$ radiation (wavelength: $\lambda = 0.1789$ nm). The scattered intensity was detected by imaging plates. The line profiles were evaluated using the Convolutional Multiple Whole Profile (CMWP) fitting procedure. In this method, the diffraction pattern is fitted by the sum of a background spline and the convolution of the instrumental pattern and the theoretical line profiles related to the crystallite size, dislocations and twin faults. The details of the procedure are available elsewhere [11].

3. Results and discussion

The results of the mechanical tests carried out on the industrially rolled materials are shown in **Figure 5**. Similar data for the materials rolled in laboratory have been published in [8]. Caliber rolling performed in laboratory [8] resulted in a slightly higher strength and a similar ductility compared to the process carried out under industrial conditions.

The reason for the slightly better mechanical performance of the material rolled in the laboratory can be attributed to a more rigorous control of the thermo-mechanical conditions (e.g. the temperature of the sample) during the manufacturing process.

Caliber rolling both in laboratory and industrial environments yielded about two times larger strength than that for the initial annealed state. The parameters characterizing the

ductility do not show uniform tendencies. The elongation to failure slightly decreased due to rolling while the reduction of area remained unchanged within experimental error. At the same time, the strain energy density to fracture increased to more than twice the value characteristic of the initial state. This can be attributed to much larger flow stress values for the rolled specimens. The various industrially manufactured samples show slightly different mechanical performances (see **Figure 5**) which can be attributed to the deviations in the processing conditions.

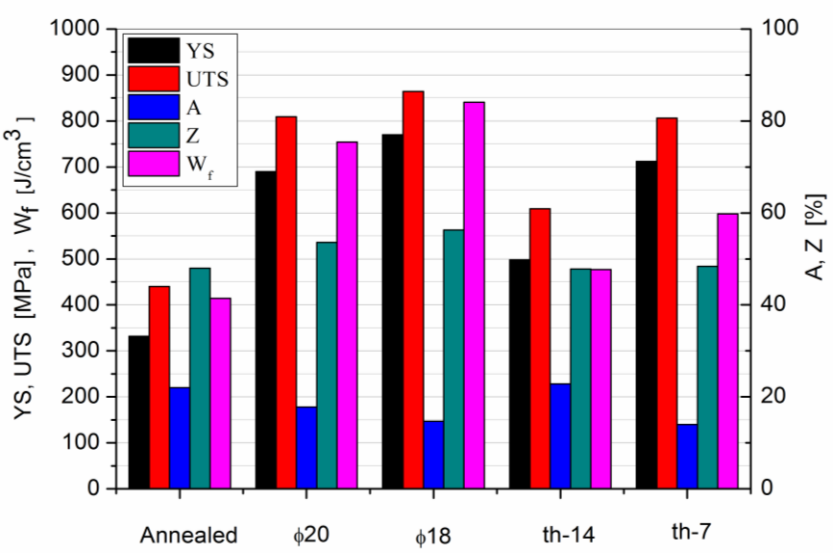

Figure 5. Mechanical properties of industrially rolled titanium samples. YS: yield strength, UTS: ultimate tensile strength, A: elongation to failure, Z: reduction in area, W_f: strain energy density to fracture. The experimental error of the values is about 8 %. ϕ20: sample from product 1, ϕ18: sample from product 2, th-14: sample from product 3, th-7: sample from product 4 (see **Table 4**).

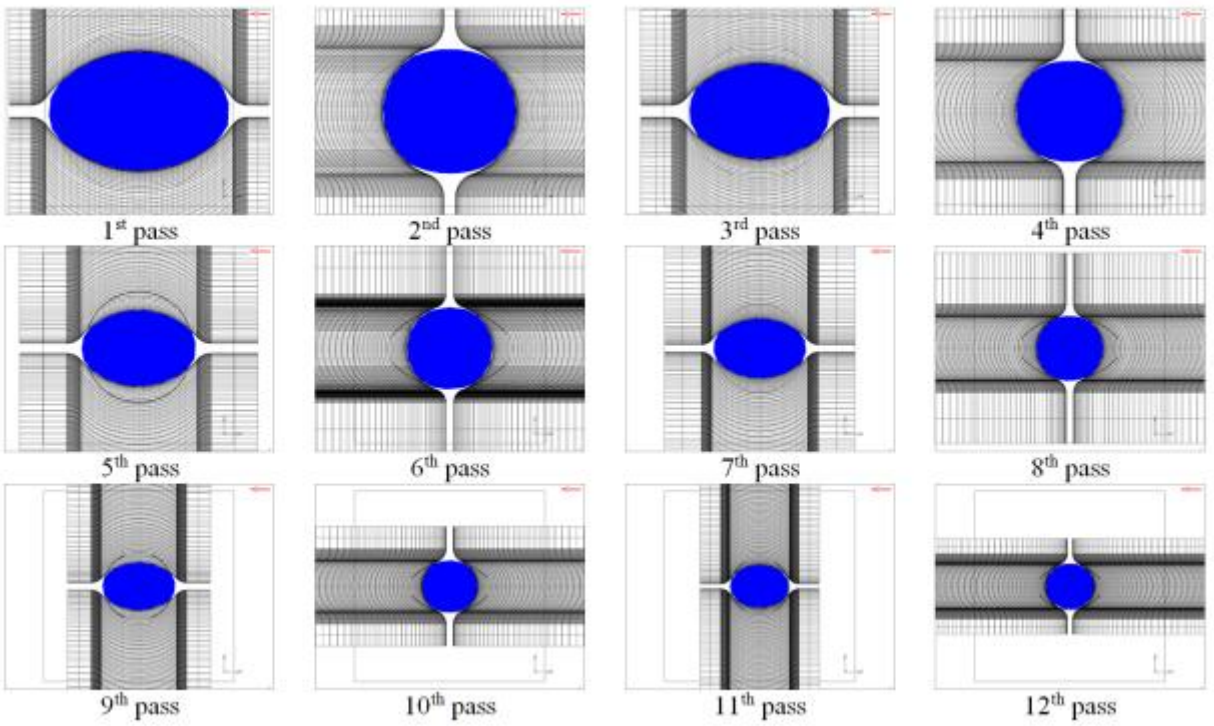

Figure 6. Roll cavity filling during industrial caliber rolling as shown by FEM analysis.

The progress of the industrial caliber rolling process obtained by FEM analysis is illustrated in **Figure 6**, where roll cavity filling is shown for different rolling passes. **Figure 7** shows the total plastic strain and the parameter of non-monotonicity at five different points in the sample. The locations of these points on the cross-section of the initial rod are shown at the upper left corner in **Figure 7**. Both the strain and the parameter of non-monotonicity change mainly when the rods travel through the roll cavities. The total strain increases with increasing the duration of caliber rolling in all points and it reaches a value of about 3.5 – 5.1 at the end of deformation. The degree of non-monotonicity first increases up to about 1.5, then it varies between 1.2 and 2 for long rolling times. *NM* has considerably higher values than one which indicates a non-monotonic nature of deformation in industrial caliber rolling.

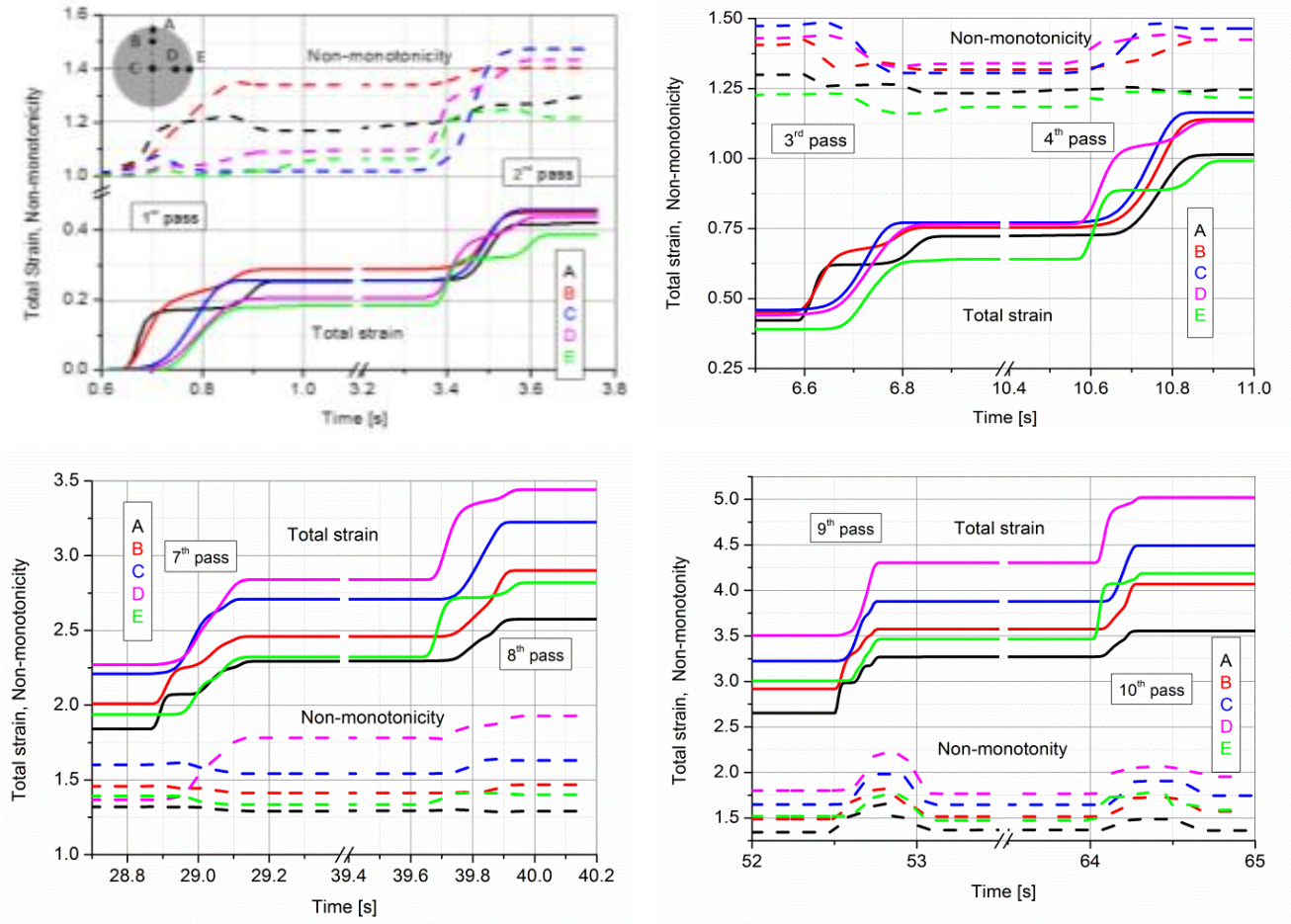

Figure 7. Changing of the total strain and the parameter of non-monotonicity at points A, B, C, D and E during industrial rolling.

In the FEM analysis the components of the logarithmic deviatoric strain tensor were determined which gave the components of the strain vector. The evolution of these components were visualised as rolling proceeds in **Figure 8**. It is revealed that considerable shear strains are developed during caliber rolling which most probably resulted in a grain refinement during deformation.

TEM images (not shown here) revealed that the grain size in the initial Ti material was between 1 and 4 μm. Rolling in laboratory yielded significant grain refinement down to the UFG regime, as illustrated in the TEM images of **Figure 9**, obtained at the end of the

manufacturing process. In the cross-section the average grain size was about 300 nm. In the longitudinal section the grains were elongated with an average width and length of 300 nm and 1 μm, respectively. Electron diffraction patterns for the specimen rolled in laboratory are also presented in the insets of **Figure 9**. The transition from a spotted to a ring-like diffraction pattern due to rolling also confirms the strong grain-refinement.

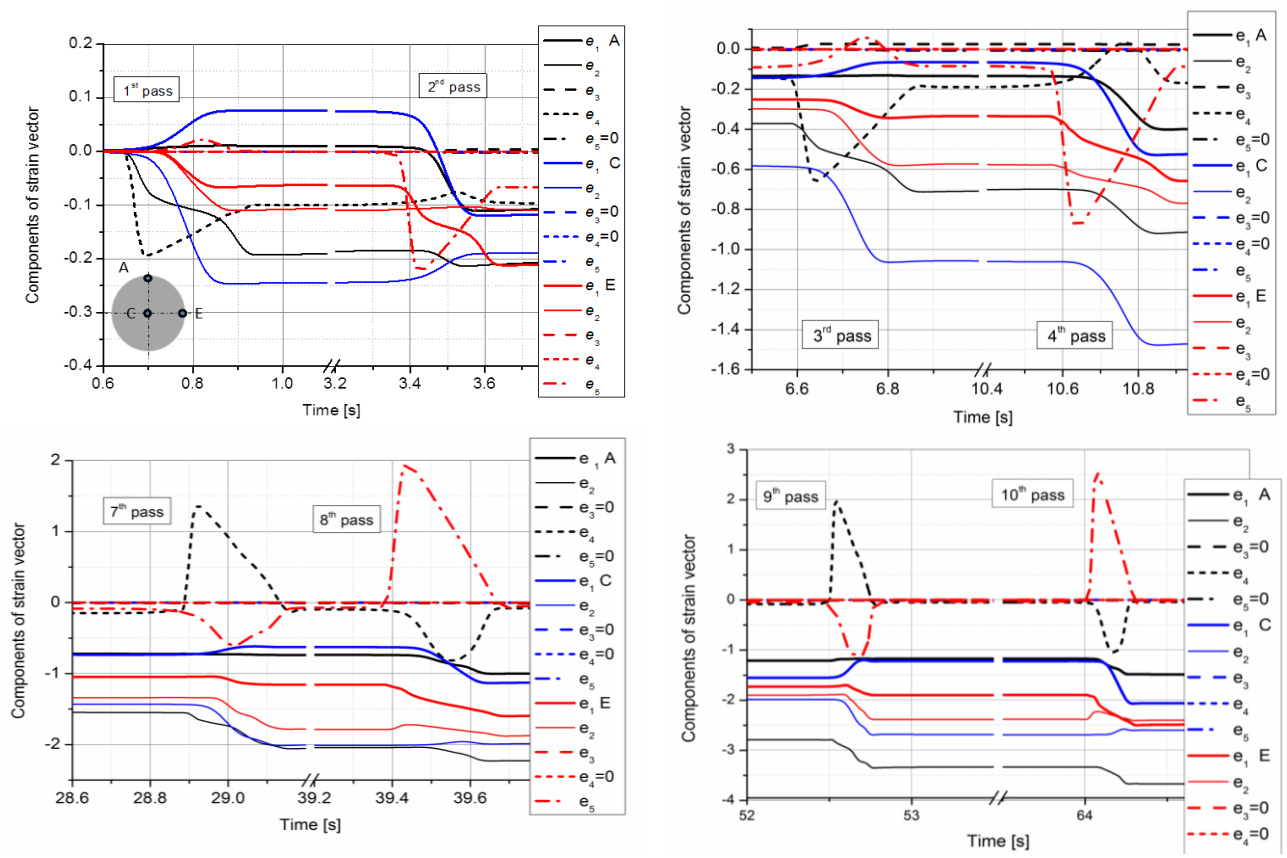

Figure 8. Changing the components of the strain vector at points A, C and E during caliber rolling.

After industrial rolling the grains are also elongated in the longitudinal section, as revealed in **Figures 9** and **10**. The average width and the length of the grains are 500 nm and 1 μm, respectively. In the cross-section, considerable elongation of the grains was not observed. In this section the mean grain size is 500 nm. It can be concluded that both laboratory and industrial rolling procedures resulted in UFG microstructures, but the grain refinement was slightly stronger in the former case, as also indicated by the electron diffraction patterns. The smaller grain size can explain the slightly higher strength of the material rolled in laboratory. It is noted that the grain size obtained on the cross-section of the sample rolled in laboratory (300 nm) is close to the value (265 nm) determined for Ti processed by eight passes of ECAP at 400 – 450 °C and subsequently rolled at room temperature to a total strain (reduction in cross-section area) of 73 % [12].

The crystallite size and the dislocation density were determined on the longitudinal sections by X-ray line profile analysis. The average crystallite sizes determined by X-ray line profile analysis (62 and 127 nm for the laboratory and industrial rolling processes, respectively) are smaller than the grain size values obtained by TEM, which has already been observed for other plastically deformed metals [13].

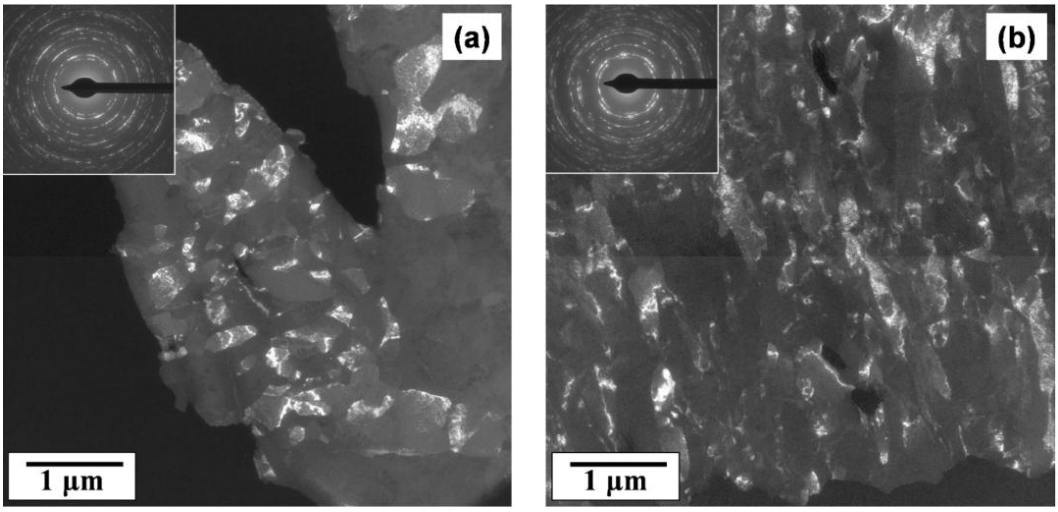

Figure 9. Dark field TEM images of the grain structure in laboratory rolled Grade 2 titanium. (a) cross- and (b) longitudinal sections. The rolling direction is vertical in figure (b).The insets show the corresponding diffraction patterns

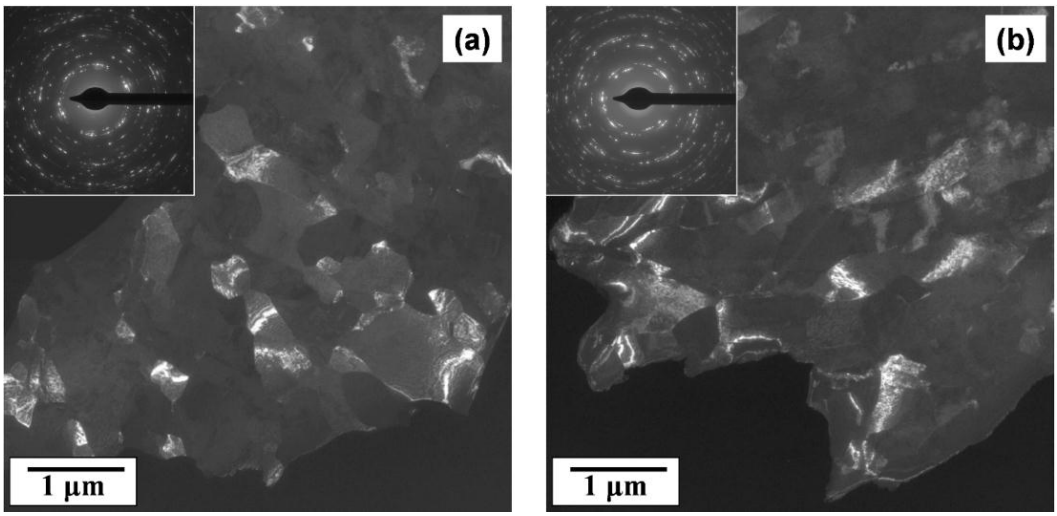

Figure 10. Dark field TEM images of the grain structure in industrially rolled Grade 2 titanium. (a) cross- and (b) longitudinal sections. The rolling direction is vertical in figure (b).The insets show the corresponding diffraction patterns.

This phenomenon can be attributed to the fact that the crystallites are equivalent to the domains in the microstructure which scatter X-rays coherently. As the coherency of X-rays breaks even if they are scattered from volumes having quite small misorientations (1 – 2 °), the crystallite size corresponds rather to the subgrain size in severely deformed microstructures [13]. The dislocation density increased to 4.7 and $3.9 \cdot 10^{14}$ m^{-2} during laboratory and industrial rolling processes, respectively. The reduction in the crystallite size and the increment in dislocation density are stronger in the laboratory rolling procedure, but the difference between the dislocation densities obtained by the two types of rolling is not very large.

4. Conclusions

1. It was shown that warm caliber rolling carried out on Grade 2 titanium at about 450 °C in laboratory yielded an UFG microstructure with high strength and good ductility.
2. Finite element modelling confirmed the non-monotonic nature of caliber rolling which is necessary for the production of a fine-grained structure.
3. Caliber rolling carried out in industrial environment yielded similar small grain size and improved mechanical properties as the process performed in laboratory. It was proposed that this technology might be a candidate process for mass-production of UFG titanium with high strength and good ductility. This may open a new gate to commercialization of SPD-processed materials.

Acknowledgements

This study was supported by the Hungarian Scientific Research Fund, OTKA, Grant Nos. K 100500 and K 109021.

References

1. Y. Saito, H. Utsunomiya, N. Tsuji, T. Sakai. Novel ultra-high straining process for bulk materials – Development of the accumulative roll-bonding. Acta Materi., 1999, 47, 2, 579-583.
2. N. Tsuji, Y. Saito, S.-H. Lee, Y. Minamino. Accumulative roll-bonding and other new techniques to produce bulk ultrafine grained materials. Adv. Engi. Mater., 2003), 5, 5, 338-344.
3. A. Ma, Y. Nishida, K. Suzuki, I. Shigematsu, N. Saito. Characteristics of plastic deformation by rotary-die equal-channel angular pressing. Scripta Mater., 2005, 52, 6, 433-437.
4. R. Z. Valiev, T. G. Langdom. Principles of equal-channel angular pressing as a processing tool for grain refinement. Prog. Mater. Sci., 2006, 51, 881-981.
5. A. P. Zhilyaev, T. G. Langdon. Using high-pressure torsion for metal processing. Fundamentals and applications. Progr. Mater. Sci., 2008, 53, 893-979.
6. J. Huang, Y. T. Zhu, D. J. Alexander, X. Liao, T. C. Lowe, R. J. Asaro. Development of repetitive corrugation and straightening. Mater. Sci. & Eng.A, 2004, 371, 35-39.
7. G. A. Smirnov–Aljajev. Resistance of Materials to Plastic Deformation. 1978, Leningrad, Mashinostroenie.
8. G. Krállics, J. Gubicza, Z. Bezi, I. Barkai. Manufacturing of ultrafine-grained titanium by caliber rolling in the laboratory and in industry. J. Mater. Proc. Technol., 2014, 214. 1307-1315.
9. A. A. Ilyushin. Continuum Mechanics. 1990, Moscow, Moscow Univ. Press.

10. G. Krállics, D. Malgyn. Finite element simulation of equal channel angular pressing. In: Severe Plastic Deformation: Towards Bulk Production of Nanostructured Materials (Ed. A. Burhanettin). 2005, New York: Nova Sci. Publ. Inc., 445-464.
11. G. Ribárik, J. Gubicza, T. Ungár. Correlation between strength and microstruc-ture of ball milled Al–Mg alloys determined by X-ray diffraction. Mater. Sci. & Eng. A, 2004, 387-389, 343-347.
12. Y. T. Zhu, J. Y. Huang, J. Gubicza, T. Ungár, Y. M. Wang, E. Ma, R. Z. Valiev. Nanostructures in Ti processed by severe plastic deformation. J. Mater. Res., 2003, 18, 1908-1917.
13. J. Gubicza, T. Ungár, Characterization of defect structures in nanocrystallinematerials by X-ray line profile analysis. Zeitschrift fur Kristallographie, 2007, 222, 567-579.